Progress In Electromagnetics Research B, Vol. 32, 149–167, 2011

STUDIES ON THE DYNAMICS OF BILATERALLY COUPLED X-BAND GUNN OSCILLATORS

B. C. Sarkar[1, *], D. Sarkar[2], S. Sarkar[3], and J. Chakraborty[1]

[1]Department of Physics, Burdwan University, India

[2]Department of Electronics and Telecommunication Engineering, Jadavpur University, India

[3]Electronics Department, Burdwan Raj College, India

Abstract—The dynamics of a system comprising of two bilaterally coupled Gunn oscillators (BCGOs) has been examined using a circuit theoretic model of the Gunn oscillator (GO). The effects of coupling factors (k_{ij}) between i-th and j-th oscillators on the frequency-range of synchronized operation and the magnitude of common frequency of oscillation have been examined semi-analytically and by numerical solution of the system equations. The occurrence of chaotic oscillations at the verge of synchronization bands is observed in numerical simulation. The experimental response of the BCGO operating in the X-band is obtained and the results are found to be qualitatively similar to the analytical and numerical predictions.

1. INTRODUCTION

The phenomenon of coupled oscillations have become a problem of active research in several branches of physical, biological and social sciences [1–3] in recent years. It has opened up application potential of coupled oscillators in several interesting fields. But at the same time a complete understanding of the dynamics of such systems is a formidable problem from analytical point of view. In electronic engineering in general and communication technology in particular, the importance of coupled oscillators has been underscored by several researchers [4–7], as they are useful in the problems related to stable signal generation and synchronous amplification in RF and Microwave (MW) communication systems.

Received 22 May 2011, Accepted 6 July 2011, Scheduled 12 July 2011

* Corresponding author: Bishnu Charan Sarkar (bcsarkar_phy@yahoo.co.in).

Use of Gunn diode based oscillators as low noise coherent receivers, active transmitting antennas, lock-in amplifiers etc is well known [9–12]. However, like any other electronic oscillator, a single GO has inherent problems of frequency drifting and spectral broadening around the average oscillating frequency which result in phase noise and real-time amplitude instability. To overcome such problems, a number of methods like unilateral and bilateral injection synchronization of two signal sources have been suggested in the literature [13–16]. In unilateral coupling, a stable external signal having relatively narrow spectral width is injected to the target oscillator whose spectral purity is to be enhanced [13]. However if these two oscillators have nearly equal spectral characteristics, unilateral coupling would hardly serve the purpose of improving spectral purity. In that situation, use of bilateral coupling between two such oscillators can provide the desired performance. Here a fraction of the output of any one of the two oscillators is injected at the other oscillator of the system. Depending upon the amount of coupled signal and the relative phase of the two oscillator-outputs, the dynamics of the arrangement shows several interesting features. There could be a synchronized state between two oscillators for a certain range of oscillator parameters and coupling coefficients. Also, for some other conditions, nonlinear dynamical response like chaos could be observed.

In this paper, our aim is to study the dynamics of BCGO for two reasons:

(i) To find out the stable or synchronized mode of oscillation of the system; this would provide the information regarding a stable, spectrally pure signal source out of two moderately stable oscillators.

(ii) To explore the regions of unstable and/or chaotic mode of oscillation; this would provide a method of generation of microwave frequency chaotic signals from practical off-the-shelf GOs.

Generation of microwave frequency chaotic signals using Colpitts oscillators, CMOS structures and Phase-locked loops has been reported in the literature [17–22]. These signals find application in chaotic UWB RADAR and other broad-band communication systems. The BCGO studied in this paper can also be a useful source of controllable chaotic signals.

The paper has been organized in the following way. Section 2 describes the system under study and proposes a suitable circuit theoretic model of it. The equivalent circuit has been used to formulate a set of coupled differential equations for the BCGO. Section 3 presents a simplified analysis to obtain an expression for the synchronization

band (SB) as well as the common frequency of oscillation of the BCGO in terms of the coupling coefficients and other parameters. In Section 4, the system equations are numerically solved. The solutions give the ranges of SB and the conditions of chaotic oscillation of the system under study for different values of oscillator and coupling parameters. Description of the experimental setup and the results obtained thereof are given in Section 5. Implications of these observations and scope of future works in these directions have been provided in Section 6.

2. DERIVATION OF SYSTEM EQUATIONS

Figure 1 shows the simplified functional structure of BCGO. Here two GOs (GO-1 and GO-2) are connected in a closed loop structure with the help of two circulators (CR-1 and CR-2) and two attenuators (ATN-1 and ATN-2). Since GO is a one-port system, a circulator is necessary to apply the external signal to it and to take out the output signal from it. As such the GOs are connected to port-2 of the respective circulators. The signal to be injected to a GO is applied at port-1 and the output of the GO is taken out from port-3 of the respective circulators. As shown in Figure 1, ATN-1 (ATN-2) connects port-3 of CR-1 (CR-2) to port-2 of CR-2 (CR-1). The coupling strengths between the two GOs are adjusted by the respective attenuators. k_{12} (k_{21}) represents the coupling factor (CF) between GO-1 (GO-2) and GO-2 (GO-1) adjusted by ATN-1 (ATN-2). The output of GO-1 is observed with the help of a spectrum analyser (SA).

Now we discuss the method of obtaining a circuit-theoretic equivalent model of a single GO as well as a BCGO system. A Gunn diode is a two terminal semiconductor device where a piece of bulk III-V semiconductor material is sandwiched between two electrodes (Figure 3(a)). The volt-ampere characteristic of a practical Gunn-diode used in GO (Model. No. X2152) is experimentally obtained

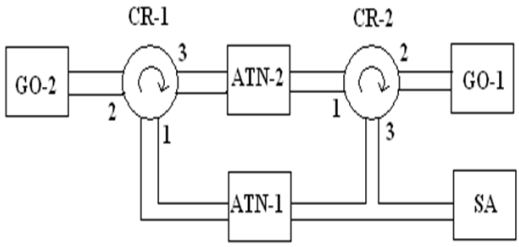

Figure 1. Simplified functional structure of BCGO.

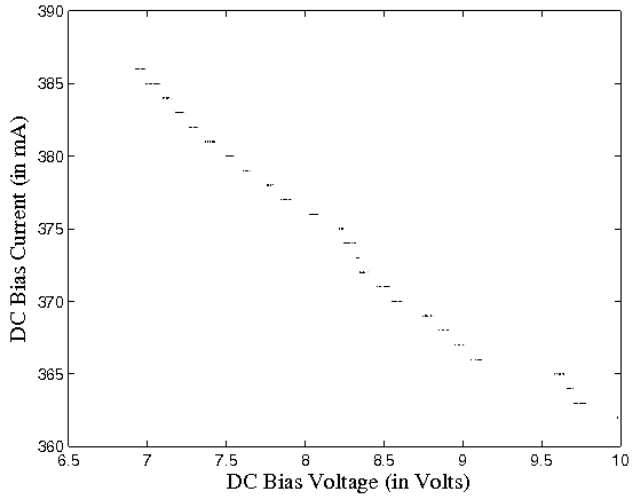

Figure 2. Experimentally obtained v-i characteristics of Gunn diode in negative resistance region.

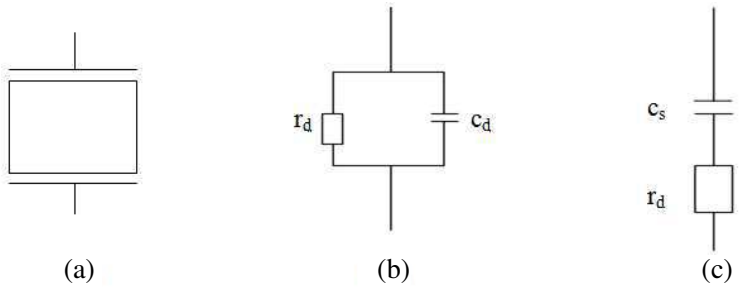

Figure 3. (a) Schematic diagram of Gunn diode; (b) Parallel equivalent circuit; (c) Series equivalent circuit.

and is shown in Figure 2 for anode voltage above the critical voltage of the diode. In this region the diode current decreases non-linearly with the increase of diode voltage. Thus in this region, the equivalent circuit of a Gunn diode can be taken as a parallel combination of a nonlinear negative resistor (r_d) and a capacitor (c_d) as shown in Figure 3(b). This parallel form is equivalent to a series combination of the same resistor (r_d) and another suitable capacitor (c_s) for which the diode admittance remains unchanged at the frequency of interest. This is shown in Figure 3(c). Here r_d and c_s both are nonlinear voltage dependent device parameters [8, 10].

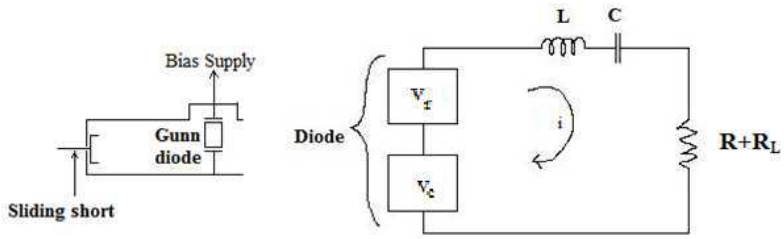

Figure 4. (a) Schematic diagram of Gunn diode oscillator; (b) Series equivalent circuit.

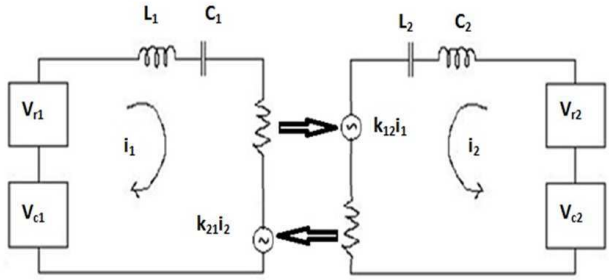

Figure 5. Equivalent circuit of BCGO.

A practical microwave GO is designed by mounting this diode within a waveguide cavity as shown in Figure 4(a). According to the principle of operation of a GO, the negative resistance of the properly biased Gunn diode compensates the loss of the resonant cavity to produce oscillation. The frequency of oscillation would be determined by the combined inductive and capacitive parameters of the cavity and the diode. The oscillator can be mechanically tuned by varying the location of the shorting plunger of the wave guide cavity with the help of a micrometer screw fitted with it. The GO can also be electrically tuned by varying the dc bias of the Gunn diode. The equivalent circuit of the GO is shown in Figure 4(b). Here R, L and C represent respectively the resistive, inductive and capacitive parts of the cavity impedance; R_L represents the external load connected with it. Since r_d and c_s are both nonlinear in nature, the voltage drops v_r across r_d and v_c across c_s would be nonlinear functions of the instantaneous current $i = \frac{dq}{dt}$ and instantaneous charge q respectively.

Considering up to the cubic nonlinearity term and remembering that the device offers negative resistance, v_r and v_c are expressed as follows:

$$v_r = -\beta_1 i + \beta_3 i^3 \tag{1}$$

$$v_c = -\alpha_1 q + \alpha_3 q^3 \tag{2}$$

Here β_1, β_3, α_1 and α_3 are the device parameters and their magnitude would depend on the dc bias point. Now applying Kirchhoffs Mesh law in Figure 5, one can write the system equation of the GO operating in the free running condition as follows:

$$L\frac{di}{dt} + (R + R_L)i + \frac{1}{C}\int i \cdot dt + v_r + v_c = 0 \tag{3}$$

Using (1) and (2), (3) can be rewritten in the normalized form as:

$$\frac{d^2q}{d\tau^2} = aq - bq^3 + c\frac{dq}{d\tau} - d\left(\frac{dq}{d\tau}\right)^3 \tag{4}$$

Here, τ is the normalized time ($\tau = \omega_r t$), where $\omega_r = \frac{1}{\sqrt{LC}}$ represents the resonant frequency of the cavity. a, b, c and d are circuit parameters associated with the properties of the active device and the waveguide cavity. They are represented in (5) to (8).

$$a = \alpha_1 C - 1 \tag{5}$$

$$b = \alpha_3 C \tag{6}$$

$$c = \frac{\beta_1 - R - R_L}{\omega_r L} \tag{7}$$

$$d = \frac{\beta_3 \omega_r}{L} \tag{8}$$

The dynamics of a single free-running GO can be studied using the system Equation (4).

Now in the system of BCGO, a fraction of the output of a GO is injected into the other GO. This can be circuit theoretically modeled by including an additional voltage source in the equivalent circuit of particular GO. This voltage source in the equivalent circuit of GO-1 (GO-2) is to be taken as proportional to the current in the equivalent circuit of GO-2 (GO-1) to ensure the coupling between these two oscillators. Figure 5 shows this equivalent circuit of BCGO. Hence following (4) the system equations for GO-1 and GO-2 can be written as:

$$\frac{d^2q_1}{d\tau^2} = a_1 q_1 - b_1 q_1^3 + c_1\frac{dq_1}{d\tau} - d_1\left(\frac{dq_1}{d\tau}\right)^3 + k_{21}\left(\frac{dq_2}{d\tau} - \frac{dq_1}{d\tau}\right) \tag{9}$$

$$\frac{d^2q_2}{d\tau^2} = a_2q_2 - b_2q_2^3 + c_2\frac{dq_2}{d\tau} - d_2\left(\frac{dq_2}{d\tau}\right)^3 + k_{12}\left(\frac{dq_1}{d\tau} - \frac{dq_2}{d\tau}\right) \quad (10)$$

Here k_{21} (k_{12}) is the coupling factor (CF) in the path GO-2 (GO-1) to GO-1 (GO-2). Then solving Equations (9) and (10) for different circuit parameters and coupling factors we can study the dynamics of BCGO.

3. ANALYTICAL STUDY

3.1. Free Running Mode

The steady state amplitude and frequency of a free-running GO can be estimated by finding the solution of its system Equation (4). We take the output of GO as:

$$q(t) = A(t)\cos(\omega_0 t + \phi(t)) \quad (11)$$

Here $A(t)$, ω_0 and $\phi(t)$ are the instantaneous amplitude, angular frequency and phase of free running GO respectively. The quantities $A(t)$ and $\phi(t)$ are assumed to be slowly varying functions of time. This implies that $|\frac{dA(t)}{dt}| \ll |A(t)|$ and $|\frac{d\phi(t)}{dt}| \ll |\phi(t)|$. Now using (11) in (4) and applying the method of harmonic balance [23], one can obtain the expressions for the derivatives of instantaneous amplitude and phase equations of the free running GO as follows:

$$\frac{dA}{dt} = A\left(c - \frac{3dA^2\omega_0^2}{4}\right) \quad (12)$$

$$\frac{d\phi}{dt} = -\frac{\omega_0}{2} + \frac{1}{2\omega_0}\left(\frac{3bA^2}{4} - A\right) \quad (13)$$

At steady state condition, putting $\frac{dA}{dt} = 0$ and $\frac{d\phi}{dt} = 0$ one can obtain the implicit equations governing the relation between the free running angular frequency ω_0 and the steady state amplitude A_0 of the GO output signal as follows:

$$\omega_0 = \left(\frac{3bA_0^2}{4} - a\right)^{\frac{1}{2}} \quad (14)$$

$$A_0 = \left(\frac{4c}{3d\omega_0^2}\right)^{\frac{1}{2}} \quad (15)$$

From (14) and (15), one can derive the expression for the free running angular frequency of the GO as:

$$\omega_0^2 = \frac{a}{2}\left(\left(1 + \frac{4bc}{da^2}\right)^{\frac{1}{2}} - 1\right) \quad (16)$$

From the Equations (14) to (16), it is quite evident that the free running behaviour of the GO is controlled by the system parameters a, b, c and d.

3.2. Coupled Mode

In the BCGO, system behaviour of individual oscillators are modified from their free-running mode due to coupling with the other oscillator. Depending upon the strength of coupling, the dynamics of the system can attain any one of the following states: 1) Nearly Uncorrelated state, 2) Quasi-periodic State, 3) Mutually Synchronized State and 4) "Chaotic" state. In case-1 an individual oscillator is least perturbed by the presence of the other oscillator because of small magnitude of CFs. The spectral output of any single oscillator would show the presence of a signal of single frequency. In case-2, the output of the GOs contains signals of discrete frequencies. This is equivalent to quasi-periodic state of an unilaterally coupled injection synchronized oscillator. This state occurs when the frequencies of the interacting oscillators are incommensurate, that is the ratio of frequencies $\frac{f_2}{f_1}$ is an irrational number [25]. Case-3 mentioned above is the synchronized state or locked state of the two oscillators. Both the oscillators have a common frequency of oscillation with a relative phase shift. The range of the synchronization band (SB) is related to the magnitudes of coupling factors. It has been shown quasi-analytically below that the SB is a function of coupling factors, free-running amplitudes and frequencies of the two GOs of the coupled system. Chaotic state mentioned in case-4 is an interesting observation of the present study. For some critical values of coupling factors and oscillator parameters, the dynamics becomes apparently random. Here the spectra of both the GOs in the system show continuous broadband characteristic which is a feature for chaotic oscillations.

Now we discuss the synchronized state of the BCGO in details. Considering the synchronized mode of oscillation in the BCGO we take the solution for system Equations (9) and (10) as:

$$q_{1,2}(t) = A_{1,2}(t)\cos(\omega t + \phi_{1,2}(t)) \tag{17}$$

Substituting (17) in (9) and (10) and following some rigorous mathematical steps one obtains the amplitude and phase-equations

of GO-1 and GO-2 as follows:

$$\frac{dA_1}{dt} = \frac{A_1}{2}\left(c_1 - \frac{3d_1A_1^2\omega_1^2}{4}\right) + \frac{k_{21}}{2}(A_2\cos\Delta\phi) \tag{18}$$

$$\frac{d\phi_1}{dt} = \frac{1}{2\omega}\left(\omega_1^2 - \omega^2\right) + \frac{k_{21}A_2}{2A_1}\sin\Delta\phi \tag{19}$$

$$\frac{dA_2}{dt} = \frac{A_2}{2}\left(c_2 - \frac{3d_2A_2^2\omega_2^2}{4}\right) + \frac{k_{12}}{2}(A_1\cos\Delta\phi) \tag{20}$$

$$\frac{d\phi_2}{dt} = \frac{1}{2\omega}\left(\omega_2^2 - \omega^2\right) - \frac{k_{12}A_1}{2A_2}\sin\Delta\phi \tag{21}$$

Here ω_1 and ω_2 represent the free running angular frequencies of GO-1 and GO-2 respectively. The phase difference between two GOs is given by $\Delta\phi = \phi_2 - \phi_1$. In the steady state synchronized condition, the quantities A_1, A_2, ϕ_1 and ϕ_2 are time-invariant (having zero time-derivatives). Solving the phase Equations (19) and (21) we obtain the expression for common frequency of synchronized oscillation as given in Equation (22).

$$\omega = \left[\frac{|k_{12}|A_1^2\omega_1^2 + |k_{21}|A_2^2\omega_2^2}{|k_{12}|A_1^2 + |k_{21}|A_2^2}\right]^{\frac{1}{2}} \tag{22}$$

Also in the state of phase-synchronization between the two oscillators $\Delta\phi$ will be constant of time ($\frac{d(\Delta\phi)}{dt} = 0$). The time-rate of change of $\Delta\phi$ can be obtained by subtracting (21) from (19) as:

$$\frac{d(\Delta\phi)}{dt} = \frac{1}{2\omega}\left(\omega_2^2 - \omega_1^2\right) + (x_1|k_{12}| + x_2|k_{21}|)\sin\Delta\phi \tag{23}$$

Here we put $x_1 = \frac{A_1}{A_2}$ and $x_2 = \frac{A_2}{A_1}$. After some simplification and considering $\omega_2 + \omega_1 \approx 2\omega$, we get from (23):

$$\omega_2 - \omega_1 = (x_2|k_{21}| + x_1|k_{12}|)\sin(\Delta\phi) \tag{24}$$

This relation shows that the BCGO system would have a synchronized state with steady state phase-error $\Delta\phi_{SS}$ given by $\sin^{-1}(\frac{\omega_2-\omega_1}{|x_2k_{21}|+|x_1k_{12}|})$. Remembering the maximum value of $\Delta\phi_{SS} = \pm\frac{\pi}{2}$, the range of frequency difference between the two oscillators that maintains phase-locked condition between them depends on the magnitudes of CFs of the two paths and the relative magnitudes of the oscillator outputs. This indicates that if the system is unilaterally coupled (i.e., one of the CF is zero) the range of synchronization is broad (i.e., larger than the BCGO system).

4. NUMERICAL ANALYSIS

Equations (9) and (10) are non-autonomous nonlinear coupled second order ordinary differential equations (ODE). A complete solution of these equations is difficult to obtain, if not impossible. So, the dynamics of the BCGO is studied numerically by solving these system equations. For this purpose we decompose (9) and (10) into two pairs of first order differential equations as follows:

$$\frac{dq_1}{d\tau} = p_1 \tag{25}$$

$$\frac{dq_2}{d\tau} = p_2 \tag{26}$$

$$\frac{dp_1}{d\tau} = a_1 q_1 - b_1 q_1^3 + c_1 p_1 - d_1 p_1^3 + k_{21} p_2 \tag{27}$$

$$\frac{dp_2}{d\tau} = a_2 q_2 - b_2 q_2^3 + c_2 p_2 - d_2 p_2^3 + k_{12} p_1 \tag{28}$$

We solve Equations (25) to (28) using fourth order Runge-Kutta technique in MATLAB platform. The system response is studied by noting the time variation of $q_{1,2}$, phase plane plot of $(q_{1,2}, p_{1,2})$ and frequency components present in time varying signal (obtained by Discrete Fourier transform (DFT) of time samples of $q_{1,2}$ using MATLAB's in-built 'fft' function). To have the steady state response of the system, a sufficient number of samples of state variables $q_{1,2}$ and $p_{1,2}$ from the initial time have not been taken into account.

The following observations have been made from the numerical as well as analytical study:

- We have four parameters a, b, c and d for numerical tuning of the individual GOs. It is evident from Equations (5) and (6) that a and b are related to the capacitive part of the Gunn device as well as cavity and hence play the primary role in governing the system frequency. It is observed from (16) that sensitivity of parameter b is more compared to that of a in frequency-tuning of the GOs. Figure 6 shows the variation of angular frequency as well as amplitude of the free running GO with the parameter b. The numerically obtained values of frequency and amplitude are found to be in close agreement with the analytical results. The difference in the simulated and analytical values is due to the fact that the analytical result is based on an assumed sinusoidal solution of the system equation whereas the RK-method based simulated result provides a nearly sinusoidal solution in general. Further the analytical method considers a nearly time-independent amplitude which is somewhat approximate.

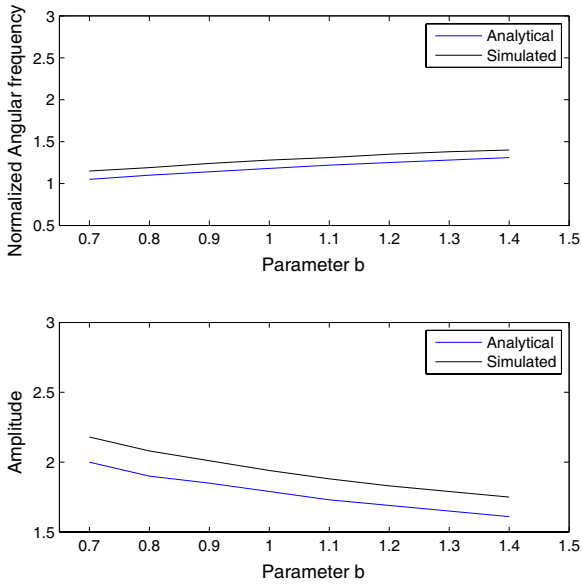

Figure 6. Variation of normalized angular frequency and amplitude of free running GO with parameter b.

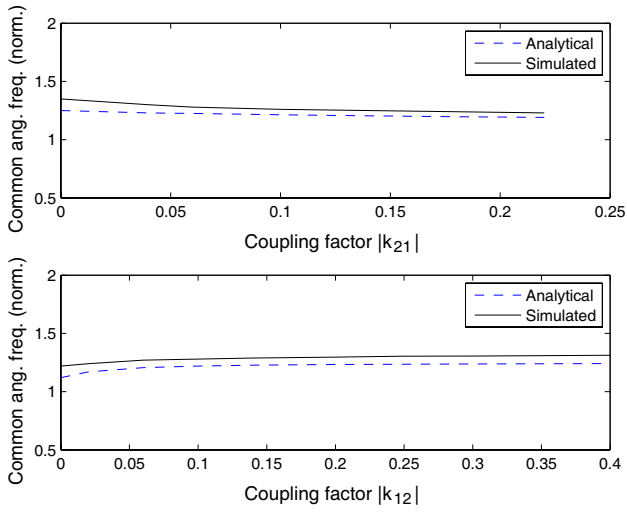

Figure 7. Variation of common frequency of the BCGO system with coupling factors $|k_{21}|$ ($|k_{12}| = 0.2$) and $|k_{12}|$ ($|k_{21}| = 0.04$) ($\omega_1 = 1.35$, $\omega_2 = 1.22$).

- Figures 7(a) and 7(b) show the variation of common frequency of oscillation ω of the BCGO system with the CFs $|k_{21}|$ and $|k_{12}|$ respectively for two GOs with fixed frequency and amplitude. We have considered $\omega_1 > \omega_2$. It has been observed that for a particular value of $|k_{21}|(|k_{12}|)$, ω is shifted from $\omega_2(\omega_1)$ to $\omega_1(\omega_2)$ as $|k_{12}|(|k_{21}|)$ increases.
  Further for a BCGO system with $\omega_1 = 1.32$, $A_1 = 1.59$, $\omega_2 = 0.95$, $A_2 = 2.21$, $|k_{12}| = 0.2$, $|k_{21}| = 0.18$ the analytical value of common frequency, as obtained from (22) is 1.22. In numerical simulation, the corresponding values of ω_1, ω_2, A_1 and A_2 are adjusted by proper selection of device parameters and then the common frequency of oscillation is obtained as 1.16. The slight difference between the two results can be explained by the similar arguments as given for a single free running GO in the previous paragraph.
- Keeping the value of k_{12} fixed, SB of the BCGO system has been calculated both analytically and numerically for different values of k_{21}. It has been observed that SB of the system increases with k_{21} (Table 1).
- Figures 8 and 9 show the simulated output spectrum of the BCGO

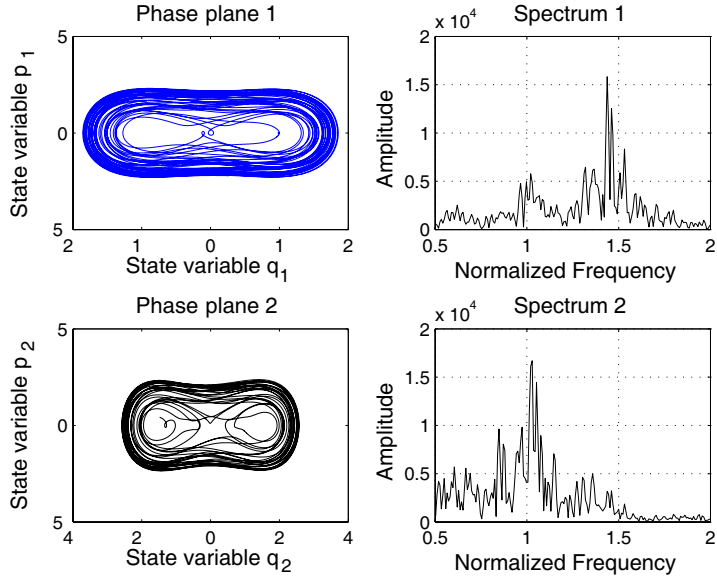

Figure 8. Output spectrum of the BCGO system: $|k_{12}| = 0.2$, $|k_{21}| = 0.2$, $\omega_1 = 1.35$, $\omega_2 = 0.94$.

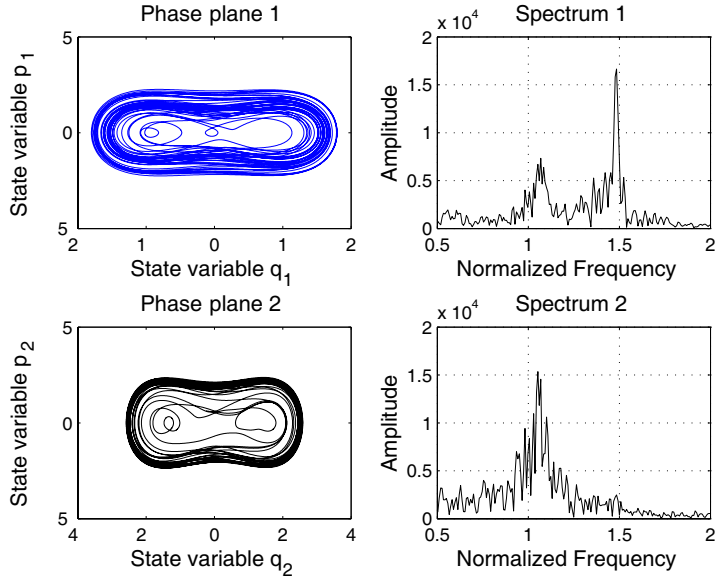

Figure 9. Output spectrum of the BCGO system: $|k_{12}| = 0.2$, $|k_{21}| = 0.18$, $\omega_1 = 1.33$, $\omega_2 = 0.95$.

Table 1. Variation of SB of BCGO System with coupling factor $|k_{21}|$.

$\|k_{12}\|$	$\|k_{21}\|$	$SB_{Simulated}$	$SB_{Analytical}$
0.2	0.18	0.371	0.38
0.2	0.2	0.385	0.40
0.2	0.22	0.412	0.42
0.2	0.24	0.425	0.44

system along with the phase-plane plots of GO output-variables for two sets of CFs when the two GOs are in out of synchronization condition. Occurrence of chaotic oscillation is evident from the broad output spectrum and the double-scroll type phase plane plot showing strange attractors.

Further, the obtained time-series data from the numerical solution of the system equations are analyzed with the help of open-source TISEAN package [26] to find out the Maximal Lyapunov exponent (MLE). It is well known that a finite positive value of the MLE is a strong evidence of chaotic state of the system [24, 25]. Our analysis of time-series data of q_1 and q_2 (shown in Figures 8 and

9 with TISEAN package gives the scaled values of MLEs as 1 and 0.5 respectively. The results prove that the system is operating in chaotic mode of oscillation.

5. EXPERIMENTAL RESULTS

To study the dynamics of the BCGO system experimentally, a hardware arrangement has been realized according to the functional block-diagram shown in Figure 1. The specifications of the active and passive components used in the experimental set-up are enlisted below:

1. GO-1 (Model No. X2152, Serial No. 1029, Bias Voltage = 9.43 Volts, Free Running frequency = 10 GHz, Output Power = 14.39 dBm)
2. GO-2 (Model No. X2152, Serial No. 1030, Bias Voltage = 9.51 Volts, Free Running frequency = 10 GHz, Output Power = 14.49 dBm)
3. CR-1 (Model No. XC621)
4. CR-2 (Model No. XC622)
5. ATN-1 (Model No. 0815)
6. ATN-2 (Model No. 0816)
7. Rhode & Schwarz Spectrum Analyser (9 kHz–18 GHz)

In the experiment the frequencies of the respective oscillators have been varied with the help of micrometer screws fitted with waveguide-type cavity resonators. Moreover the CFs between the oscillators in two paths are changed with the adjustable attenuators. The magnitude of the oscillator frequencies and CFs are taken from the calibration curve experimentally drawn beforehand.

In the first part of the experiment ATN-1 is fixed at a particular value and we measure the range of synchronization of GO-1 for different values of attenuation factor of ATN-2. The obtained results are shown in Table 2. It is observed that as GO-1 is coupled with GO-2, the SB of GO-1 increases as more power from GO-2 is fed back to GO-1, i.e., with the increase in k_{21}.

In the second part of the experiment, output spectrum of GO-1 is critically examined by varying the CFs of the two paths and frequency of GO-2. It is observed that depending upon CFs and frequency-detuning values, the output of GO-1 shows patch-like broad spectrum outside the SB of the system (Figures 10(a) and 10(b)), which indicates that the system has entered into chaotic state of oscillation.

The effect of coupling coefficients on the dynamics of the BCGO is shown in Figure 11. It depicts the output spectrum of GO-1 when

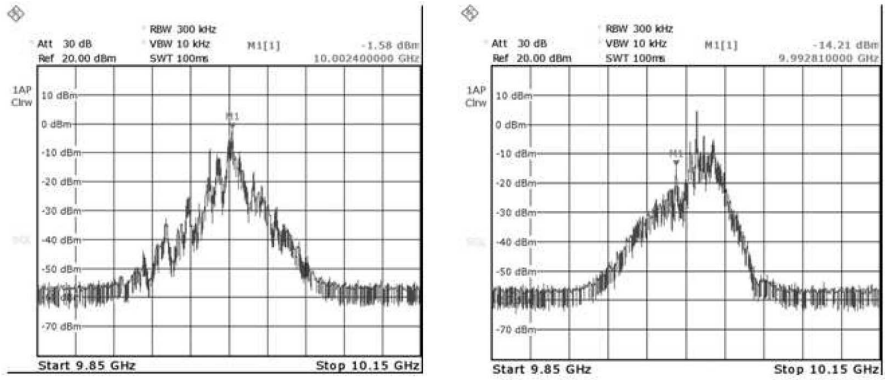

(a) (b)

Figure 10. Selected output spectra of the GO-1 in the BCGO system: (a) $|k_{12}(\exp.)| = 0.398$, $|k_{21}(\exp.)| = 0.398$, $f_1 = 10\,\text{GHz}$, $f_2 = 9.985\,\text{GHz}$; (b) $|k_{12}(\exp.)| = 0.398$, $|k_{21}(\exp.)| = 0.630$, $f_1 = 10\,\text{GHz}$, $f_2 = 10.007\,\text{GHz}$.

Table 2. Variation of SB of GO-1 in BCGO system for different injecting power (P_{in}). Here for GO-1, $P_{out} = 14.39\,\text{dBm}$ and free running frequency $= 10\,\text{GHz}$.

P_{in} (dBm)	$\lvert k_{21}\ (\exp.)\rvert$	$\text{SB}_{\exp.}$ ($\lvert k_{12}(\exp.)\rvert = 0.398$) in MHz
-13.35	0.0015	0.8
-2.75	0.017	1.8
6.4	0.01412	5.3
10.39	0.398	15.57
12.39	0.0630	20.36

k_{21} is varied keeping k_{12} fixed. With increase in the magnitude of k_{21}, the system transits from a synchronized state to a quasi-periodic state through a chaotic state. The chaotic state shown in Figure 11(b), the width of the output spectrum is about 100 MHz about the center frequency 10.012 GHz if one considers the component signal power up to 30 dBm less from obtained peak power. The spectrum of the chaotic state is distinct from that of the quasi-periodic state (Figure 11(c)) which contains discrete spectral components.

These experimental observations follow qualitatively the results as obtained from numerical analysis (Section 4) as well as in analytical study (Section 3).

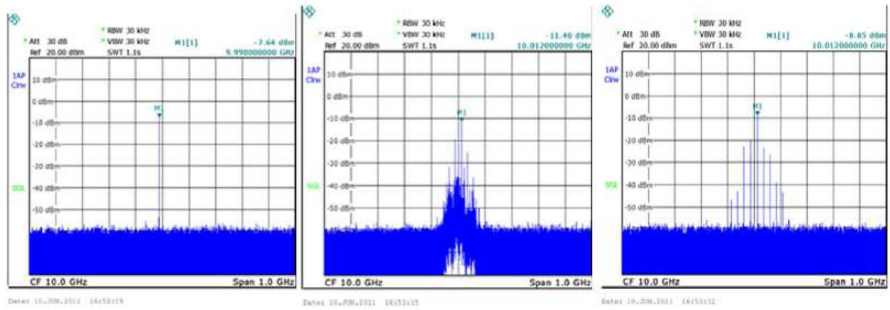

(a) (b) (c)

Figure 11. Output spectrum of the GO-2 in the BCGO system for three different states. Output powers and frequencies of GO-1 and GO-2 are respectively 14 dBm, 14.5 dBm, 10.012 GHz, 9.988 GHz. $|k_{21}(\exp.)|$ is fixed at 0.187. (a) Synchronized state: $|k_{12}(\exp.)| = 0.0398$. (b) Chaotic state: $|k_{12}(\exp.)| = 0.316$. (c) Quasi-periodic state: $|k_{12}(\exp.)| = 0.50$.

6. CONCLUSION

In this paper, the dynamics of X-band BCGO has been extensively studied through semi-analytical methods, numerical simulation as well as experimental techniques. A circuit-theoretic model of a single cavity resonator based GO has been derived at the outset. The dependence of free-running frequency and amplitude of oscillation on the circuit and device parameters has been examined through numerical simulation and the same have been compared with the analytical solutions of oscillator equations. Equivalence of two sets of results confirms the validity of the system model and its numerical simulation. Examining the physical principle of operation of the BCGO, designed using X-band circuit components, a set of coupled differential equations of the BCGO has been formulated. A detailed study of these equations through numerical simulation reveals a rich dynamics of the BCGO system for different values of CFs, oscillator free running frequencies etc. For some specific sets of CFs a frequency band of synchronized operation of the two oscillators is observed and the value of the common frequency of system oscillation is numerically obtained through DFT of the time-series data. The system equations are semi-analytically examined in the synchronized state of BCGO operation and the common frequency parameter as well as the SB are obtained. The numerical and semi-analytical results show close agreement. For specific sets of values of the CFs, the output power

spectrum of any of the oscillators in the BCGO shows a continuous broadband characteristics just outside the synchronization band of the BCGO. This nature of the oscillation spectrum is a signature of chaotic oscillations. Further, the phase-plane plots and time-series analysis of the oscillator output variables show presence of strange attractor along with finite positive maximal Lyapunov exponent which is a firm evidence of chaotic oscillations in the system. Hardware experiments done with GOs in X-band (around 10 GHz) closely support the predictions of numerical studies indicating an SB of BCGO system as well as regions of oscillations at the external boundaries of SB. Thus one can conclude that a BCGO system with suitable set of CFs could be a potential source of chaotic signals in microwave frequency range.

ACKNOWLEDGMENT

Authors (BCS,SS and JC) acknowledge partial financial assistance from DAE,BRNS (India) and DST (India) through sponsored research projects in carrying out the work. Authors thank Ms. Dia Ghosh, Ms Chaitali Kole and Mr Arun Guin for their help in carrying out the experimental studies.

REFERENCES

1. Boi, S., I. D. Couzin, N. D. Buono, N. R. Franks, and N. F. Britton, "Coupled oscillators and activity waves in ant colonies," *Proceedings Royal Society*, 371–378, London, 1998.
2. Glova, A. F., "Phase locking of optically coupled lasers," *Quantum Electronics*, Vol. 33, No. 4, 283–306, 2003.
3. Stori, D. W., et al., "Dynamics of two strongly coupled Van der Pol oscillators," *International Journal of Nonlinear Dynamics*, Vol. 7, No. 3, 143–152, 1982.
4. Anishchenko, V., S. Astakhov, and T. Vadivasova, "Phase dynamics of two coupled oscillators under external periodic force," *Europhysics Letters*, Vol. 86, 2009.
5. Ram, R. J., R. Sporer, H. R. Blank, and R. A. York, "Chaotic dynamics in coupled microwave oscillators," *IEEE Trans. Microwave Theory and Technique*, Vol. 48, 1909–1916, 2000.
6. Uwate, Y. and Y. Nishio, "Synchronization phenomena in Van der Pol Oscillators coupled by a time varying resistor," *International Journal of Bifurcation and Chaos*, Vol. 17, No. 10, 3565–3569, 2007.

7. Volos, C. K., I. M. Kyprianidis, and I. N. Stouboulos, "Experimental synchronization of two resistively coupled duffing type circuits," *Nonlinear Phenomena in Complex Systems*, Vol. 11, No. 2, 187–192, 2008.
8. Liang, L. and Z. Bo, "A new nonlinear circuit model for GaAs Gunn diode in oscillator," *8th International Symposium on Antennas, Propagation and EM Theory*, 1306–1309, 2008.
9. Bates, R. S. and S. Feeney, "Novel varactor tuned millimeter wave Gunn oscillator," *Electronics Letters*, Vol. 23, No. 14, 714–715, 1987.
10. Biswas, B. N., S. Chatterjee, S. Sarkar, A. K. Bhattacharya, and S. K. Ray, "Bias tuned injection locked discriminators," *IEEE Trans. on Microwave Theory and Techniques*, Vol. 35, No. 9, 812–818, 1987.
11. Sarkar, S., T. Banerjee, D. Mondal, and B. C. Sarkar, "Theory and performance of an electrically controlled microwave phase shifter," *Indian Journal of Pure and Applied Physics*, Vol. 43, 215–220, 2005.
12. Sarkar, S., "Structure and application of a modified lock-in notch filter using solid state microwave oscillator," *Indian Journal of Engineering and Material Science*, Vol. 1, 149–152, 1994.
13. Kurokawa, K., "Injection locking of microwave solid state oscillator," *Proc IEEE*, Vol. 61, 1386–1410, 1973.
14. Diakoku, K. and Y. Mizushima, "Properties of injection locking in the non-linear oscillator," *International Journal of Electronics*, Vol. 31, 279–292, 1971.
15. Zhu, X., Y. Chen, and W. Hong, "Q-band injection-locked Gunn diode oscillator," *International Journal of Infrared and Millimeter Waves*, Vol. 17, No. 3, 527–533, 1996.
16. Alekseev, Y. I., "Determination of basic characteristics of synchronization of Gunn self-excited oscillators," *Instruments and Experimental Techniques*, Vol. 50, No. 2, 241–243, 2007.
17. Shi, Z. G. and L. X. Ran, "Microwave chaotic Colpitts oscillator: Design, implementation and applications," *Journal of Electromagnetic Waves and Applications*, Vol. 20, No. 10, 1335–1349, 2006.
18. Qiao, S., Z.-G. Shi, T. Jiang, and L.-X. Ran, "A new architecture of UWB radar utilizing microwave chaotic signals and chaos synchronization," *Progress In Electromagnetics Research*, Vol. 75, 22–237, 2007.
19. Jiang, T., S. Qiao, Z.-G. Shi, L. Peng, J. Huangfu, W.-Z. Cui,

W. Ma, and L.-X. Ran, "Simulation and experimental evaluation of the radar signal performance of chaotic signals generated from a microwave Colpitts oscillator," *Progress In Electromagnetics Research*, Vol. 90, 15–30, 2009.

20. Nikishov, A. Y., "Generation of the microwave chaotic oscillations by CMOS structure," *PIERS Proceedings*, 457–461, Moscow, Russia, Aug. 18–21, 2009.
21. Dmitriev, A. S., A. V. Kletsov, and L. V. Kuzmin, "Experimental generation of chaotic oscillations in microwave band by phase-locked loop," *PIERS Proceedings*, 1498–1502, Moscow, Russia, Aug. 18–21, 2009.
22. Shi, Z. G., S. H. Hong, and K. S. Chen, "Experimental study on tracking the state of analog Chuas circuit with particle filter for chaos synchronization," *Physics Letters A*, Vol. 372, 5575–5580, 2008.
23. Jordan, D. W. and P. Smith, *Nonlinear Ordinary Differential Equations: An Introduction for Scientists and Engineers*, 4th edition, Oxford University Press, New York, 2007.
24. Kantz, H. and T. Schreiber, *Nonlinear Time Series Analysis*, Cambridge University Press, 2004.
25. Hilborn, R. C., *Chaos and Nonlinear Dynamics*, 2nd edition, Oxford University Press, New York, 2000.
26. Hegger, R., H. Kantz, and T. Schreiber, *TISEAN Package*, Web-address: http://www.mpipks-dresden.mpg.de/ tisean.